

聚乙烯吡咯烷酮修饰的 CdS 纳米晶:多元醇合成、表征和可见光活性

陈崇启 詹瑛瑛 郑远辉 林性贻 郑 起*

(福州大学化肥催化剂国家工程研究中心,福州 350002)

摘要: 采用溶剂热法合成了具有不同晶粒尺寸的聚乙烯吡咯烷酮(PVP)修饰的 CdS 纳米晶,并运用 XRD, N_2 物理吸附, TEM, IR, UV-Vis 等手段进行表征。结果表明,所制得的样品均为聚乙烯吡咯烷酮(PVP)修饰的 CdS 纳米晶;添加四甲基氢氧化铵(TMAH)有利于获得晶粒尺寸较小的 CdS 纳米晶;受纳米晶粒尺寸的影响, CdS 纳米晶的吸收边发生蓝移且可见光催化活性明显提高。

关键词: 溶剂热; PVP 修饰的 CdS 纳米晶; 半导体; 可见光催化

中图分类号: O614.24² **文献标识码:** A **文章编号:** 1001-4861(2008)04-0605-05

Poly(*N*-vinyl-2-pyrrolidone)-capped CdS Nanocrystals: Polyol Synthesis, Characterization and Visible-light Photocatalysis

CHEN Chong-Qi ZHAN Ying-Ying ZHENG Yuan-Hui LIN Xing-Yi ZHENG Qi*

(National Engineering Research Center of Chemical Fertilizer Catalyst, Fuzhou University, Fuzhou 350002)

Abstract: Poly(*N*-vinyl-2-pyrrolidone)-capped CdS nanocrystals with different crystalline sizes were synthesized through a simple solvothermal method. The structures of the as-synthesized samples were characterized by XRD, N_2 physisorption, TEM, IR spectroscopy, and UV-Vis spectroscopy. The results show that the as-synthesized samples are poly(*N*-vinyl-2-pyrrolidone)-capped CdS nanohybrid materials; the grain size of CdS nanocrystals is smaller when tetramethylammonium hydroxide(TMAH) is introduced in the reaction system. In addition, it is also found that the bandgap of CdS nanocrystals is blue shifted and the visible-light photocatalytic activity of the sample synthesized in the presence of TMAH increases due to the size effect.

Key words: solvothermal; PVP-capped CdS nanocrystals; semiconductors; visible-light photocatalysis

II-VI 半导体纳米材料具有新颖的物理和化学性质, 已经吸引了许多研究者的兴趣。各种纳米结构的 II-VI 半导体已经被合成用于潜在的应用在光学和光电子器件, 如发光二极管^[1], 太阳能电池^[2], 光电探测器^[3], 激光器^[4], 和传感器^[5]。许多基本性质半导体纳米材料被表达为尺寸、形状和/或缺陷, 作为

例子, 当 CdS 纳米晶的尺寸接近于 Bohr 半径的相应激子, 能带的量子化变得明显, 并且观察到光学光谱^[6]中的蓝移; 并且它已经报告了 CdS 纳米晶的新发射峰是由于它们的特殊缺陷^[7,8]。因此, 控制半导体的纳米结构将提供机会为这些材料定制性质并提供

收稿日期: 2007-10-29。收修改稿日期: 2008-01-24。

国家自然科学基金(No.20771025)和福建省重大专项项目(No.2005H201-2)资助。

*通讯联系人。E-mail: zhengqi@fzu.edu.cn; Tel: +86-59183731234-8112; Fax: +86-591-83738808

第一作者: 陈崇启, 男, 24 岁, 硕士研究生; 研究方向: 新型纳米催化材料。

possibilities for observing interesting and useful physical phenomena^[9,10].

As an n-type semiconductor with a bandgap of 2.4 eV, cadmium sulfide (CdS) can form two kinds of polymorphs: zinc-blende (cubic) and wurzite (hexagonal) structure. It has been reported that hexagonal CdS nanoparticles possess a relatively large nonlinear optical response and photocatalytic activity, having potential applications in optoelectronic devices^[11] and as hydrogen production photocatalyst^[12]. So far, various approaches have been made on the synthesis of CdS nanocrystals, which are usually fabricated from aqueous solution of cadmium salt either by reacting with an aqueous solution of Na₂S or by bubbling H₂S gas^[13,14]. However, to our best knowledge, there is little report about CdS nanocrystals synthesized by using sulfur powder as sulfur source. In addition, it is well-known that the surfactants, which can not only act as templates or structure-directing agents for inorganic materials, but also can control the nucleation and crystallization of the inorganic materials, are commonly used in controlling the growth of inorganic materials, and thus controlling their morphology and/or size^[15,16]. Herein, a facile ethylene glycol (EG) mediated solvothermal process was used to synthesize CdS nanocrystals with different sizes and morphologies in the presence of polyvinylpyrrolidone (PVP). The effect of tetramethylammonium hydroxide (TMAH) on controlling the size of nanoparticles was investigated. In addition, the microstructures, optical properties and photocatalytic activity of the as-synthesized PVP-capped CdS nanocrystals were also studied.

1 Experimental

1.1 Preparation of CdS nanocrystals

Cadmium acetate (A.R., Tianjin Fuchen Chemical Reagent Factory), sulfur powder (C.P., Tianjin Kermel Chemical Reagent Co., Ltd), ethylene glycol (A.R., Tianjin Fuchen Chemical Reagent Factory), Tetramethylammonium hydroxide solution (TMAH, 25%, Sinopharm Group Chemical Reagent Co. Ltd) and polyvinylpyrrolidone (PVP, $k=30$, A.R., Sinopharm Group Chemical Reagent Co. Ltd) were used as starting

materials without further purification. In a typical procedure, 0.266 g (1 mmol) of Cd(Ac)₂·2H₂O and 0.600 g of PVP were dissolved in 15 mL of ethylene glycol. Subsequently, 0.032 g (1 mmol) of sulfur and a certain amount of TMAH (e.g., 0 and 1 mL) were added into the above transparent solution with agitation. Then the mixture was transferred into a Teflon-lined stainless steel autoclave of 20 mL capacity and maintained at 180 °C for 5 h. When the reactions were completed, the autoclave was cooled to room temperature naturally. The resulting precipitates were collected by centrifugation, washed with pure ethanol for several times, and dried in air at 50 °C for 5 h. The obtained samples were denoted as CdS-1 (without TMAH) and CdS-2 (with TMAH), respectively.

1.2 Characterizations

The powder XRD patterns of the as-synthesized samples were recorded by a BURKE D8 X-ray diffractometer using Cu K α radiation ($\lambda=0.15418$ nm) filtering with Ni at a scanning rate of $2.4^\circ \cdot \text{min}^{-1}$ for 2θ ranging from 15° to 80° over a voltage and current of 40 kV and 40 mA utilizing scintillometer (NaI). The microstructures and morphologies of the samples were investigated by a Tecnai G2 F20 Field Emission Transmission Electron Microscope (FETEM) working at 200 kV. The surface area of the samples was measured by Brunauer-Emmett-Teller (BET) method using N₂ physisorption at 77 K on a Quantachrome NOVA 4200e apparatus. Samples were normally prepared for N₂ physisorption measurement by outgassing at 423 K under vacuum for 3 h. The hybrid chemical nature of the nanocrystals was characterized on Perkin-Elmer FTIR spectrometer by KBr method scanning from 4000 cm⁻¹ to 400 cm⁻¹. The UV-Vis spectra of the nanocrystals were measured on VARIAN Cary 50 Conc UV-Vis spectrophotometer. For photocatalytic measurement, 30 mg of each sample was suspended in 90 mL of standard methyl orange (MO) aqueous solution ($5.0 \times 10^{-5} \text{ mol} \cdot \text{L}^{-1}$), subsequently, the mixture was put in quartz tube and agitated for 0.5 h in the absence of light. After that, the mixture was irradiated by visible irradiation, using a 500 W tungsten halogen lamp (Philips), positioned inside a cylindrical Pyrex vessel surrounded by a

circulating water jacket to cool the lamp. A cutoff filter was also placed outside the Pyrex jacket to remove the radiation below 420 nm, ensuring the reaction system to be irradiated only by visible light wavelengths. The distance between the mixture and the lamp is about 8 cm. After a given irradiation time, about 5 mL of the mixture was withdrawn and the catalysts were separated from the suspensions by centrifugation. The photocatalytic degradation process was monitored by UV-Vis spectrophotometer (Perkin-Elmer Lambda 950) (measuring the absorption of MO at 463 nm).

2 Results and discussion

2.1 Synthetic mechanism of CdS nanocrystals

It is well known that grain sizes of inorganic materials are greatly dependent on their nucleation and growth rate, which can be controlled by adjusting experiment parameters such as concentration of reactants and/or reaction temperature. In our work, it is expected to control the morphology and size of CdS nanocrystals by controlling the concentration of reactants (i.e., $c_{\text{Cd}^{2+}}$ and $c_{\text{S}^{2-}}$) during the reaction processes. The main reactions can be expressed as follows:



A weak reducing agent (ethylene glycol) and organic alkali (TMAH) were used to control the concentration of S^{2-} (eq.1) and Cd^{2+} (eq.2), respectively. Based on the above equations, it is reasonable that the smaller grain size of CdS nanocrystals should be obtained when TMAH is introduced in the reaction system.

2.2 XRD, nitrogen adsorption and TEM characterizations of PVP-capped CdS nanocrystals

The XRD patterns of the as-prepared samples are shown in Fig.1. All the diffraction peaks are in good agreement with the hexagonal CdS phase (PDF: 41-1049). No characteristic peaks of any other inorganic impurities such as cubic CdS phase are detected in these patterns. In addition, it is easy to find that the diffraction peaks of CdS-1 (Fig.1a) are stronger and

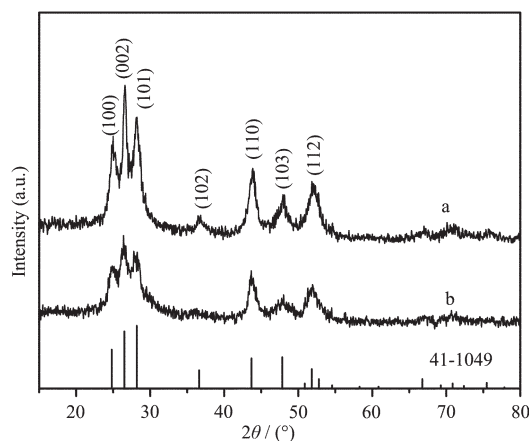


Fig.1 XRD patterns of the as-prepared samples:
(a) CdS-1 and (b) CdS-2

narrower than that of CdS-2 (Fig.1b), indicating that the CdS-1 has a larger crystalline size. In order to obtain more quantitative information of the grain size, the crystal size of the as-synthesized CdS nanocrystals is calculated by the Debye-Scherrer formula^[17]

$$L = 0.9 \lambda / (B \cdot \cos \theta) \quad (4)$$

using the full width at half maximum (FWHM) of (100), (101) and (112) planes. In the case of spherical crystallites, the relation between L and D (D : diameter of the crystallite) is given by^[18]:

$$L = (3/4) D \quad (5)$$

On the basis of the equations (4) and (5), the calculated grain sizes of CdS-1 and CdS-2 are 13.4 nm and 10.9 nm, respectively. The BET surface area of these two samples is 9.3 and 43 $\text{m}^2 \cdot \text{g}^{-1}$, respectively, further confirming the smaller grain size of CdS-2.

The TEM results of the as-prepared PVP-CdS nanocrystals are shown in Fig.2. In the system without TMAH, three-dimensional spherical CdS aggregates sized about 200 nm was obtained (Fig.2a). An enlarged TEM image (Fig.2b) from the edge of one spherical aggregate reveals that CdS spheres are composed of smaller grains with size in the range of 10~15 nm, which is in good agreement with the XRD analysis. However, when TMAH was added in the synthetic system, many small CdS nanoparticles with the diameter of 5~10 nm were formed, and some of them aggregated into larger particles without special morphology, as shown in Fig.2c. Fig.2d is a typical high-resolution TEM (HRTEM) image of a CdS-2

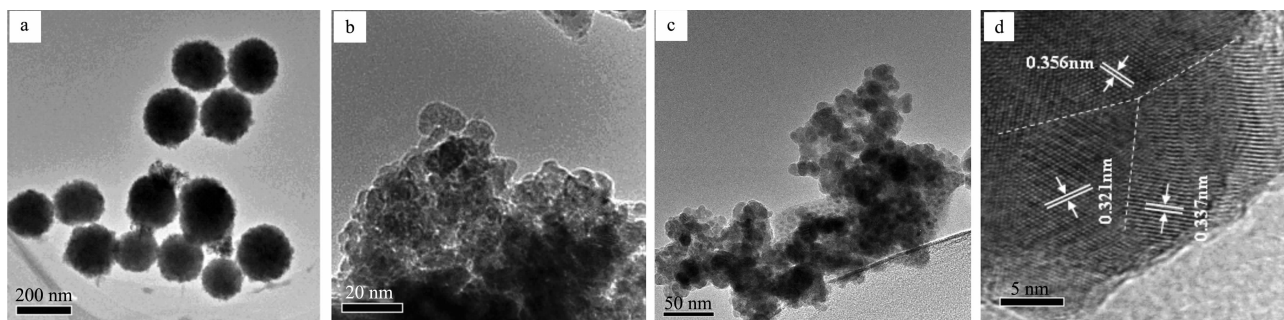


Fig.2 TEM and HRTEM images of the as-prepared samples: (a, b) CdS-1; (c, d) CdS-2.

particle. It also shows that the larger CdS aggregate is formed due to aggregation of several smaller nanograins. Meanwhile, some interfaces are easily found in Fig.2d, as highlighted by dash lines. And the spacings between adjacent lattice fringes of the nanoparticles are 0.321 nm, 0.337 nm and 0.356 nm, which are close to the d-spacing of (101), (002) and (100) planes of hexagonal CdS, respectively.

2.3 Surface structure of PVP-capped CdS nanocrystals

FTIR spectra (Fig.3) confirm the hybrid chemical nature of the as-synthesized samples. From Fig. 3, one can see that there is a broad absorption band at $\sim 3450\text{ cm}^{-1}$ for each sample, which is assigned to the hydroxyl groups of chemisorbed and/or physisorbed H_2O molecules on the surface of the corresponding samples. The absorption peaks at 1115 cm^{-1} and 1128 cm^{-1} in spectra (a) and (b) are due to bond vibration of CdS^[19], and the others are ascribed to PVP. Furthermore, it is obvious that the position of $\nu_{\text{as}}(\text{C}=\text{O})$ (1653 cm^{-1}) shifts,

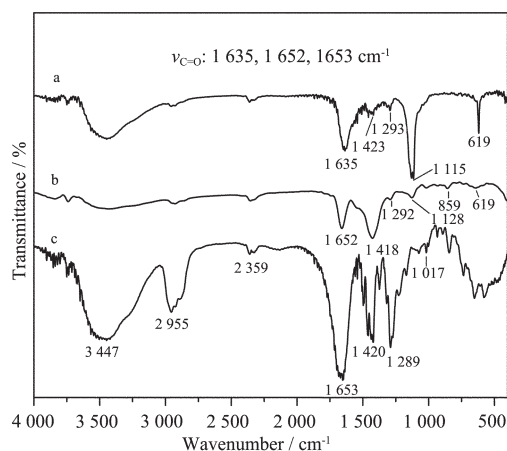


Fig.3 FTIR spectra of the as-prepared samples and PVP from the range of $4000\text{ cm}^{-1}\sim 400\text{ cm}^{-1}$: (a) CdS-1, (b) CdS-2, and (c) PVP.

which is believed to be due to the formation of coordinate bond between the PVP and CdS nanocrystals. Therefore, it is concluded that PVP molecules are chemically bonded to the surface of the as-synthesized CdS nanocrystals.

2.4 Optical properties of PVP-capped CdS nanocrystals

Fig.4 shows the UV-Vis absorption spectra of the as-synthesized PVP-capped CdS nanocrystals, whose optical band gap are determined by the following equation (eq.6) using the direct transition method^[20-22].

$$(\alpha h\nu) = A(h\nu - E_g)^{n/2} \quad (6)$$

As seen in the figure inserted in Fig.4, it is obviously that the band edge of CdS-2 blue shifts comparing with that of CdS-1, indicating the smaller grain size of CdS-2 nanocrystals, as is in good agree with the above XRD, BET and TEM results.

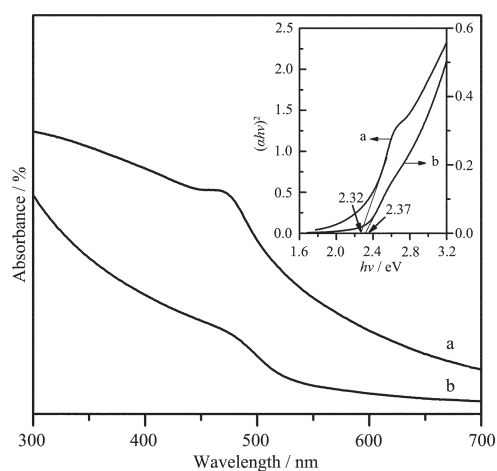


Fig.4 UV-Vis absorption spectra of the as-synthesized samples: (a) CdS-1 and (b) CdS-2.

2.5 Photocatalytic activity of CdS under visible light irradiation

Fig.5 shows time profiles of C/C_0 under visible

light irradiation, where C_0 and C are the initial concentration after the equilibrium adsorption and the reaction concentration of MO, respectively. As seen in Fig.5, the photocatalytic activity of CdS-2 nanocrystals is much higher than that of CdS-1. Based on the above XRD, N_2 -physisorption TEM, and UV-Vis absorption results, it is concluded that the particle size of CdS-2 is smaller than that of CdS-1. Therefore, it is reasonable that the higher photocatalytic performance of CdS-2 should be due to its smaller particle size.

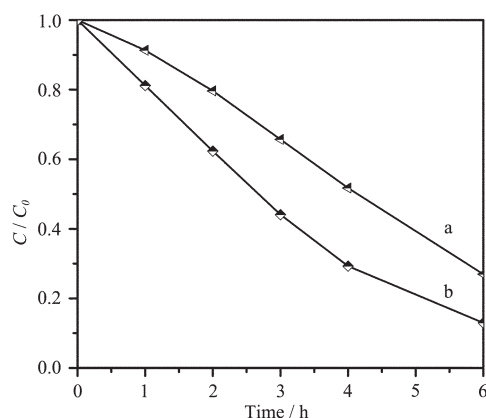


Fig.5 Photocatalytic activity of the CdS nanocrystals:
(a) CdS-1 and (b) CdS-2.

3 Conclusion

PVP-capped CdS nanocrystals with different crystal sizes were synthesized through a simple solvothermal method. It is found that the grain size of CdS nanocrystals decreases when TMAH is introduced in the reaction system. In addition, the shift of absorption edge and enhancement of visible-light photocatalytic activity of the as-synthesized CdS nanocrystals are due to the size effect.

Acknowledgments: The authors thank Prof. YANG Xiao-Hua and ZHENG Chun-Ming from Instrumentation Analysis and Measurement Center of Fuzhou University for the TEM measurement.

References:

- [1] Hayden O, Greytak A B, Bell D C. *Adv. Mater.*, **2005**,**17**(6): 701~704
- [2] Visoly-Fisher I, Cohen S R, Cahen D, et al. *Appl. Phys. Lett.*, **2003**,**83**(24):4924~4926
- [3] Kouklin N, Menon L, Wong A Z, et al. *Appl. Phys. Lett.*, **2001**, **79**(26):4423~4425
- [4] Chan Y, Steckel J S, Snee P T, et al. *Appl. Phys. Lett.*, **2005**, **86**(7):073102(3pages)
- [5] Alivisatos P. *Nat. Biotechnol.*, **2004**,**22**(1):47~52)
- [6] Jamali S, Zad ESI, Shayesteh S F. *Syn. React. Inorg. Met.*, **2007**,**37**(5):381~386
- [7] Xiong S L, Xi B J, Wang C M, et al. *Chem. Eur. J.*, **2007**,**13**(11): 3076~3081
- [8] Pattab M, Amma B S, Manzoor K, et al. *Sol. Energ. Mat. Sol. C.*, **2007**,**91**:1403~1407
- [9] Chowdhury P S, Ghosh P, Patra A. *J. Lumin.*, **2007**,**124**:327 ~332
- [10] Shieh F, Saunders A E, Korgel B A. *J. Phys. Chem. B*, **2005**, **109**:8538~8542
- [11] Peng X, Schlamp M C, Kadavanich A V, et al. *J. Am. Chem. Soc.*, **1997**,**119**:7019~7029
- [12] Jing D, Guo L. *J. Phys. Chem. B*, **2006**,**110**:11139~11145
- [13] Deng D, Yu J, Pan Y. *J. Colloid. Interf. Sci.*, **2006**,**299**:225 ~232
- [14] Zhang H, Yang D, Ma X, et al. *Mater. Lett.*, **2005**,**59**:3037 ~3041
- [15] Tian Z R, Liu J, Voigt J A, et al. *Nano Lett.*, **2003**,**3**:89~92
- [16] Lai J, Shafi K V P M, Ulman A, et al. *J. Phys. Chem. B*, **2005**,**109**:15~18
- [17] Guinier A. *X-ray Diffraction*. San Francisco: CA, **1963**.
- [18] Li H, Zhu Y, Chen S, et al. *J. Solid State Chem.*, **2003**,**172**: 102~110
- [19] Yu S, Shu L, Yang J, et al. *Nanostruct. Mater.*, **1998**,**10**: 1307~1316
- [20] Butler M A. *J. Appl. Phys.*, **1977**,**48**:1914~1920
- [21] Kyung Moon Choi, Shea K J. *J. Phys. Chem.*, **1994**,**98**:3207~ 3214
- [22] Lin X, Huang T, Huang F, et al. *J. Phys. Chem. B*, **2006**,**110**: 24629~24634